

Possibilities to modify the properties of the AW7075 aluminum alloy for the automotive industry

ARTICLE INFO

Received: 5 June 2023
Revised: 1 August 2023
Accepted: 5 August 2023
Available online: 11 January 2024

The paper investigated the AW7075 aluminum alloy that is used in the automotive industry. The alloy is widely used, among others, in the production of heads and engine blocks. The possibility of obtaining various properties of the alloy (material states) by appropriate heat treatment (saturation and aging) was demonstrated. The results of strength, hardness, abrasion, and fracture toughness tests of the alloy in the T73, RRA, and HTPP aging treatments, in comparison with the T651 reference state, are presented. The need to select the appropriate parameters of heat treatment in relation to the load conditions of the structural element, especially in elements with notches, was indicated. Depending on the state of the AW7075 alloy, the results prove the wide and diverse possibilities of its use and should be used consciously in the design and production processes of modern automotive drivetrain components.

Key words: AW7075 aluminum, aging treatments, abrasion resistance, fracture toughness, cracking mechanism in the PSS

This is an open access article under the CC BY license (<http://creativecommons.org/licenses/by/4.0/>)

1. Introduction

Present efforts to reduce emissions of internal combustion engines while at the same time increasing the efficiency of drive units have placed ever higher demands on the structural materials used in their production, which is of particular importance on a large-series scale and in the context of the selection of appropriate materials. It can be said that the producers of steel and aluminum-containing alloys strive for the widespread use of their materials for structural elements [22]. Apart from steel, aluminum alloys are a group of basic structural materials that, in light of the aforementioned current trends in the development of drive units, are once again gaining importance. They are used for the construction of engines and in the load-bearing components of motor vehicles, such as pistons [10], that require the use of materials with a low specific weight and a sufficiently high strength. Reducing the weight of vehicles is necessary to reduce fuel consumption and thus reduce the emission of toxic exhaust components [22].

Among the aluminum alloys, the following are most commonly used: 6061-T6, 2024-T5, and 7075-T6. Each has slightly different properties: 6061 is easy to weld and anodize and inexpensive, 2024 has greater strength and machinability, but the high copper content makes it difficult to anodize and weld. Compared to these two, 7075 has the highest strength (which, however, decreases at high temperatures) but is difficult to weld.

AW7075 aluminum alloy is used primarily in the basic T651 state, in turn ensuring maximum strength properties. This material is characterized by high strength, while at the same time maintaining good fracture toughness and corrosion resistance, despite the fact that maximum (static) strength is often achieved at the expense of both fracture toughness and stress corrosion cracking resistance [6]. Although this alloy has been used in the aerospace and automotive industries since the 1940s, work is still underway to modify its structure, mechanical properties, and resistance to intergranular corrosion through precise heat

treatment [24]. Research is also conducted in the field of weldability and other methods of joining, which further expands the possibilities of using this alloy [6]. It has recently been shown that the course of metallurgical processes, including the times of soaking, solution treatment, and aging of the AW7075 alloy, affects the value of tensile strength, microstructure, and corrosion resistance. For T6-temper treatment in the pre-deformed condition, it has been proved that a short time of solution heat-treatment soaking causes a decrease of the elongation at fracture [18]. These properties are the most important with regard to the application of AW7075 in the automotive industry.

7075 aluminum is used in the production of motor vehicles for both covers and mechanism housings, as well as for heavily loaded mechanical and thermal applications: slide bearings caps, heads, connecting rods [1], and the blocks of internal combustion engines [2, 19], including engines used in motorsport [14]. Rose et al. [16] even developed a model using an aluminum composite with silicon carbide as a material for an automotive camshaft. Based on the numerical analysis, they obtained results showing that the Al-SiC composite camshafts have good strain and stress characteristics and can be a good alternative to chilled cast iron and carbon steel camshafts. Sachar et al. [21] demonstrated the suitability of aluminum alloys for the construction of cylinder block fins. The low self-weight of this material reduces the weight of the engine and increases its efficiency. Besides, it provides a better coefficient of heat removal from the engine than materials such as cast iron, copper, or magnesium.

At the same time, in the case of significant loads combined with the influence of friction, there are problems with AW7075 wear in the long term due to the load and strength of the surface layer [6]. There are also reports of fatigue damage to the tested material.

In addition, classic methods of surface finishing of engine structures, such as cylinder honing [8], require good machinability and abrasion of the material. All this makes

operations modifying the AW7075 alloy, which will give it optimal properties for a given application, become very important.

The treatment that modifies the properties of the material is primarily heat treatment. For the AW7075 alloy, three aging treatments (states) other than T651 can be considered: T73 (Overaging treatment), RRA (Retrogression and Reaging), and HTPP (High-Temperature Pre-Precipitation). Each treatment is obtained by a slightly different method of solution treatment and aging (Table 1), which affects the degree of precipitate dispersion and the mechanical properties of the alloy, including fatigue strength [5, 9]. For example, it was found that the rate of fatigue cracking decreases with decreasing size of precipitates [4]. Trdan et al. [21] have also shown that the microstructure of aluminum alloys strongly affects the direction and propagation of a fatigue crack in welded joints.

However, the influence of temperature and aging time on the mechanical properties of the material is not unambiguous. Although aging at a lower temperature generally increases the effect of precipitation hardening, it turns out that for short aging times, this effect may be stronger if it takes place at higher temperatures (Fig. 1) [12, 15]. Therefore, experimental research is particularly valuable when optimizing the heat treatment process.

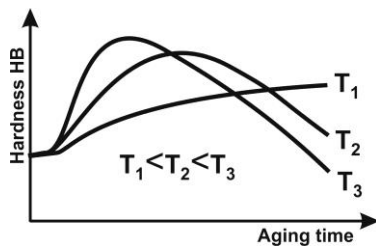


Fig. 1. The influence of temperature and aging time on the hardness of the Al-Cu alloy [12]

A large dispersion of precipitates increases the hardness, strength, and yield stress of aluminum alloys [15]. Such properties, on the one hand, have a positive effect on fatigue strength because the formation of permanent deformations in the structure is hindered (hence the use of surface work in fatigue working elements) [23]. On the other hand, however, they reduce the resistance to temporary cracking, which occurs with regard to the existing crack (notch) [7]. This paradox may be explained by the description of fracture mechanics presented in Fig. 2.

During cracking, the plastically deformed areas formed in the outer zones of the crack surface (the so-called shear lips) have the ability to stop the development of the crack, which is brittle in the inner zone. The extent of the slip lips is greater if the material is easier to be plasticized. As a result, elements made of high-strength materials have a lower fracture toughness (K_{IC} or δ_c) than those made of materials with higher plasticity (Fig. 3).

The graph shown in Fig. 3 shows another regularity: the fracture toughness decreases significantly with the increase of the thickness (B) of the fractured element. This effect must be taken into account in the design and selection of material for structural elements.

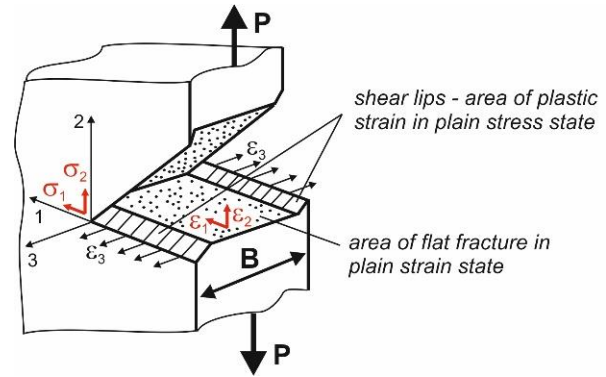


Fig. 2. Systems of strain and stress states on the fracture surface [23]

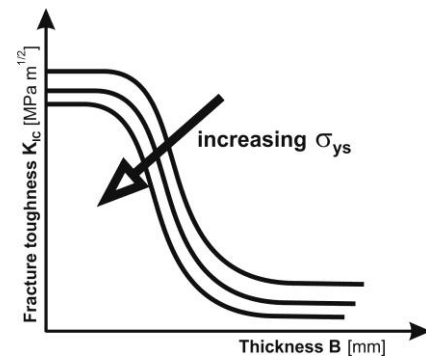


Fig. 3. The influence of yield stress on fracture toughness [15]

The presented theory was confirmed by the results of strength and the fracture toughness tests of various states of the AW 7075 material. In addition to them, hardness, microhardness, and abrasion resistance tests were also performed, which are also important in the selection of the optimal material for automotive constructions. The results of these studies are presented in the next chapter.

2. Materials and methods

The primary material for the tests was AW7075 in four states: T651, T73, RRA, and HTPP. The last three are modifications of the material properties in the basic T651 state and are most often applied in industry (Table 1) [11]. Strength tests (tensile tests), hardness tests (Brinell and Vickers methods), fracture toughness tests (CTOD tests), and abrasion wear resistance tests were carried out for the conditions mentioned above.

The static tensile tests at ambient temperature were performed on three samples from each state. Typical cylindrical, proportional test pieces were prepared with the diameter $d=6$ mm and the gauge length $L_0 = 30$ mm, which were tested in the rolling direction on an Instron 5982 testing machine with a force range of 100 kN.

The Brinell hardness test was carried out for all states on the samples intended for the CTOD test in accordance with the requirements of the standard [14] and used the ZwickRoell ZHU testing machine and a ball indenter with a diameter of 2.5 mm. The machine acted under the load of 187.5 kg applied for 15 seconds. Measurements were carried out in the central parts of the front surfaces of compact samples that did not undergo plastic deformation during the fracture toughness tests. The average values of three measu-

rements were determined for each of the samples (macrohardness).

CTOD tests were carried out on compact samples with a thickness of $B = 25$ mm, which were loaded with tensile fatigue along the rolling direction (Fig. 4a) on an MTS 810 hydraulic pulsator with a range of 250 kN. The tests were conducted to ascertain the occurrence of scrap and to determine the critical value of crack opening δ_c in accordance with the requirements of the standard [20].

Microhardness was determined by the Vickers method using the Opti MMX-X7B hardness tester with a diamond indenter in the form of a square pyramid and a load of 300 g applied for 15 seconds. The measurements were carried out in the middle of the zones of occurrence of plastic deformations caused by fatigue load on the side surfaces (sections) of the samples and after the CTOD test. Mean values from three measurements were determined for each of the samples. The results obtained in this way (microhardness) were converted to the HBW scale in order to compare them with the results of hardness measurements (macrohardness).

The resistance to abrasive wear tests of the AW7075 aluminum during friction were performed on the T-07 tribotester in accordance with the requirements of GOST 23.208-79. The tests were performed under constant load conditions of $F = 44$ N, and alumina particles (grain size #90) as required by the standard "Bonded Abrasives (...)" (ISO 8486-2:2007) were used. The test method is described in detail in [3]. In accordance with the requirements of the standard for materials with a hardness below 400 HV, each test lasted 10 minutes, which corresponds to 600 abrasive cycles. Two samples for each of the considered AW7075 aluminum were tested. The samples had dimensions of

$30 \times 30 \times 3$ mm and were taken from the plane across the thickness of the compact samples intended for the CTOD test. Values of the abrasive wear resistance rates (K_b) were determined using the weight wear method, which involves determining the difference in the mass of the sample before and after the test of abrasion, according to the relationship:

$$K_b = \frac{Z_{ww}}{Z_{wb}}$$

where Z_{ww} – mass loss of the reference specimen [g] – the standard sample i.e. aluminum in the T651 state, Z_{wb} – mass loss of the test sample [g].

The mass loss on the actual friction path was also determined for all the samples subjected to abrasion. Sample weights were determined using Sartorius Extend laboratory scales with an accuracy of 0.0001 g.

3. Results

Table 1 summarizes the heat treatment conditions performed in order to obtain the four tested states of the AW7075 aluminum and also the results of the hardness determined in the tests.

Table 2 shows the basic strength parameters obtained in the tests. The values of $R_{p0.2}$, R_m , and δ_c for the AW7075 material in the T73, RRA, and HTPP aging treatments were referred to the properties in the T651 (reference) aging treatment. The results of the abrasion resistance and cracking resistance tests, according to the CTOD test, were also collected. They were compared, as in the case of the strength results, to the parameters of the material in the T651 aging treatment.

Table 1. Heat treatment processes applied to the AW7075 aluminum alloy and material hardness

Aging state	Applied heat treatment		Hardness	
	solution	aging	Macrohardness HBW (% value relative to T651)	Microhardness HBW (% value relative to T651)
T73	470°C, 1 h, cooling – cold water	120°C, 24 h, 160°C, 30 h	152 (90%)	169 (99%)
RRA	470°C, 1 h, cooling – cold water	120°C, 24 h, 203°C, 10 min, 130°C, 18 h	172 (102%)	180 (106%)
HTPP	470°C, 1 h, 445°C, 0.5 h, cooling – cold water	120°C, 24 h	171 (101%)	171 (101%)
T651	material as supplied: solution treated, stretch relieved and artificially aged		169 (100%)	170 (100%)

Table 2. Obtained results of the experimental tests: the strength test in relation to abrasion resistance and crack resistance according to the CTOD test

Aging state	Strength properties (along the rolling direction)		Abrasive wear resistance		Fracture toughness according to the CTOD test
	$R_{p0.2}$ [MPa] (% value relative to T651)	R_m [MPa] (% value relative to T651)	abrasion resistance coefficient K_b [-] (% value relative to T651)	weight loss due to friction [mg/m] (% value relative to T651)	δ_c [mm] (% value relative to T651)
T73	484 (89%)	543 (91%)	1.22 (122%)	1.13 (82%)	0.035 (219%)
RRA	441 (81%)	497 (83%)	1.08 (108%)	1.27 (92%)	0.047 (294%)
HTPP	508 (94%)	571 (95%)	1.00 (101%)	1.37 (99%)	0.023 (144%)
T651	542 (100%)	600 (100%)	1.00 (100%)	1.38 (100%)	0.016 (100%)

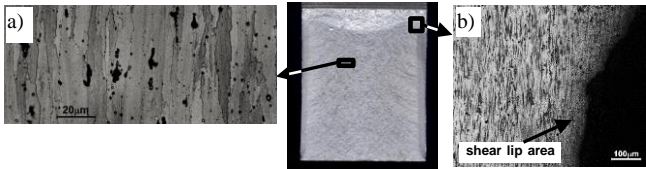


Fig. 4. Structure of the grain on the fracture surface of the AW7075-T7 compact specimen: in the middle of the flat fracture with the rolling direction indicated (a), the edge-side area with plastic strain on the shear lip (b)

4. Results analysis

The tested states of the AW7075 aluminum are characterized by very similar hardness values, with the exception of the T73 aging treatment, in which case the hardness decreased by 10% when compared to the delivery state (Table 1). However, the microhardness increases in the zone of plastic deformation and the strain hardening mechanism (noticeable in the case of RRA and HTPP aging treatments) – an increase of 11% and nearly 5%, respectively. This becomes particularly important in the case of the occurrence of material fatigue loads.

The results of the strength tests show a decrease in the value of the yield strength of each of the states of the material after heat treatment (T73, RRA, and HTPP) when compared to the T651 aging treatment (taken as the reference state). Such a modification of mechanical properties during cracking causes a greater extent of the plasticization zone in the slip lips that are formed on the edges of the crack surface. This is indicated by the greater microhardness of the material in these zones in the RRA and HTPP aging treatments (Table 2), and by the microscopic observation of the grain structure (Fig. 4b). Since the material in the slip lip zones has the ability to deform in the direction perpendicular to the direction of cracking (Fig. 2a, direction of axis 3), there is a triaxial strain state, and therefore also a plane stress state (PSN). The developing process of plastic deformation absorbs a significant part of the energy transferred to the structure by the work of external forces, which results in stopping the cracking process. This translates directly into higher fracture toughness results obtained in the CTOD tests: the best fracture toughness was shown by the material in the RRA aging treatment. It was lower for the T73 and HTPP aging treatments and the lowest in the T651 state (Table 2).

The inhibition of crack development in plastically deforming near-surface zones is also confirmed by macroscopic observations of the surface of the fatigue fractures of the compact samples, which can be seen in the photographs of the specimens (Fig. 5–6). Figure 5 shows successive stages of fatigue crack formation in the samples from the RRA, T73, and HTPP aging treatments' shear lip zone. Such an effect is clearly less visible in the T651 samples (Fig. 6).

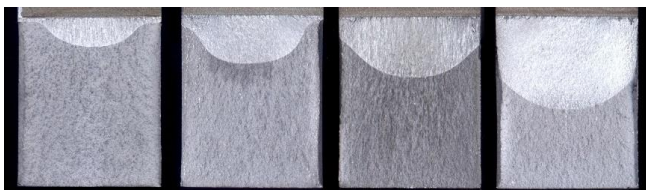


Fig. 5. Propagation of cracks in the AW-7075 material: cracks stopped by shear lips in the RRA, T73, and HTPP aging treatment

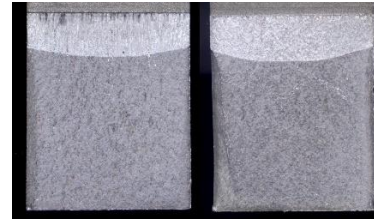


Fig. 6. Flat cracking in the T651 treatment, where the influence of shear lips is much less visible

The determined parameters, which represent resistance to abrasive wear, clearly indicate a significant increase in wear resistance in friction conditions. This is especially the case in the T73 aging treatment, despite its reduced hardness, and also in the case of the RRA aging treatment (the value of the K_p coefficient increases by 22 and 8%, respectively, and the loss of weight by 18% and nearly 8% respectively, when compared to the generally applicable T651 aging treatment).

The obtained decrease in the yield strength and hardness values as a result of heat treatment, especially visible for the RRA state, proves the weakening of the precipitate strengthening mechanism in the AW7075 material. This is a result of the increase in the size of the second phase precipitates during annealing and aging of the material. Such precipitates, however, increase the cracking resistance of the material, stopping the development of fatigue cracking for some time [17], which can be seen in the SEM photograph shown in Fig. 7. This effect is caused by the lack of coherence between the structure of the matrix and the precipitate, as a result of which an additional strong field of internal compressive stresses is created in front of the crack tip, forcing the crack to change the propagation plane.

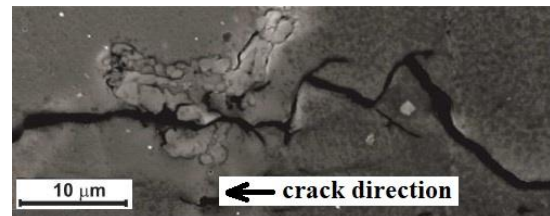


Fig. 7. Fatigue crack arrest mechanism by a second phase intermetallic precipitate in AW7075 material [17]

5. Conclusions

The results of the conducted research show that:

- the AW7075 alloy, which is a high-strength material, gains an improvement in crack resistance in notched structural elements through appropriate heat treatment, in turn resulting in greater ductility as a result of natural aging; this is indicated by the results of strength tests for the AW7075 material in the RRA and T73 aging treatments, which had the lowest yield strength $R_{p0.2}$ when compared to the reference T651 aging treatment, and the highest fracture toughness δ_c ;
- the positive effect of material plasticization on fracture toughness seen in the tests applies to cases of cracking of elements with notches; a different relationship is obtained for fatigue strength, which increases with an increasing yield point of the material;

- as a result of the tests, it was found that the material in the T73 aging treatment has the best abrasion resistance;
- when using the AW7075 material for structural elements, the nature of the work and the range of loads should be taken into account. Moreover, the heat treatment (saturation and aging) should be controlled in order to obtain the desired strength properties, abrasion resistance, fatigue strength, and crack resistance.

It should be noted that the requirements for structural elements should not always prioritize maximum short-term strength, as high-strength materials have a limited and sometimes significantly lower fracture toughness. In applications where this parameter is crucial (mainly in elements with structural notches), a material with increased plastic

properties should be selected at the expense of a slight reduction in strength parameters.

Detailed use of the results of this work belongs to the designers of structural elements. If they decide on the AW 7075 alloy, they should be aware that through appropriate heat treatment, the strength and resistance properties of this material can be modified to some extent. Each of the elements made of the AW 7075 alloy, examples of which are shown in Chapter 1, requires separate consideration in terms of strength requirements and hazards resulting from the presence of notches, temperature influence, dynamic loads, etc.

Continuation of the research may contribute to fuller use of the advantages of the AW7075 alloy, which is increasingly used in the automotive industry.

Nomenclature

PSS plane stress state
T73, RRA, T651, HTPP aging treatments
T73 overaging treatment

RRA retrogression and reaging
HTPP high-temperature pre-precipitation
T651 solution heat-treated, artificially aged, permanent set

Bibliography

- [1] Ahmed S, Khany S, Shareef S. Design, fabrication and analysis of a connecting rod with aluminum alloys and carbon fiber. *International Journal of Innovative Research in Science, Engineering and Technology*. 2014;3(10):16674-16687. <https://doi.org/10.15680/IJRSET.2014.03100036>
- [2] Aneesh T, Pawan K, Mohan L, Krisna PH, Hotta TK, Mohantu CP et al. Exploring casting defects of AA7075 alloy in the gravity die casting simulation of an IC engine block. *P I Mech Eng E-J Pro*. 2022;236(4):1556-1565. <https://doi.org/10.1177/09544089211073296>
- [3] Białobrzeska B, Kostencki P. Abrasive wear characteristics of selected low-alloy boron steels as measured in both field experiments and laboratory tests. *Wear*. 2015;328-329:149-159. <https://doi.org/10.1016/j.wear.2015.02.003>
- [4] Broek D, Bowles CQ. The effect of cold deformation and ageing on fracture crack propagation and residual strength of 2024 sheet material. NLR-TR 69048 U; 1969.
- [5] Chruścielski G, Korusiewicz L. The role of second phase intermetallic precipitates in fatigue fracture mechanism for aluminium alloy AW 7075. *Key Eng Mat*. 2013;592-593:809-812. <https://doi.org/10.4028/www.scientific.net/KEM.592-593.809>
- [6] Czapczyk K. Research on the mechanical and tribological properties of the nanocomposite Ni-P/Si₃N₄ coating deposited by chemical reduction on the AW-7075 aluminum alloy used for machine parts. Doctoral dissertation. Poznań 2019.
- [7] German J. Fundamentals of fracture mechanics. Publishing House of Cracow University of Technology. Cracow 2011.
- [8] Gruszka J, Suchecki A. New methods of internal combustion engine cylinder surface forming. *Combustion Engines*. 2007;130(3):26-34. <https://doi.org/10.19206/CE-117322>
- [9] Hahn CT, Simon R. A review of fatigue crack growth in high strength aluminium alloys and the relevant metallurgical factors. *Eng Fract Mech*. 1973;5(3):523-540. [https://doi.org/10.1016/0013-7944\(73\)90038-6](https://doi.org/10.1016/0013-7944(73)90038-6)
- [10] Iskra A, Babiak M, Kałużny J. The influence of applying a layer of carbon nanotubes on the piston bearing surface on friction losses. *Combustion Engines*. 2014;159(4):26-31. <https://doi.org/10.19206/CE-116927>
- [11] Jin-Feng L, Zhuo-Wei P, Chao-Xing L, Zhi-Qiang J, Wen-Jing C, Zi-Qiao Z. Mechanical properties, corrosion behaviors and microstructures of 7075 aluminium alloy. *T Nonferrous Metal Soc*. 2008;18:755-762. [https://doi.org/10.1016/S1003-6326\(08\)60130-2](https://doi.org/10.1016/S1003-6326(08)60130-2)
- [12] Łatkowski A, Jarominek J. Metal science of non-ferrous metals. Publishing House AGH University of Krakow. Krakow 1994.
- [13] Magnus Billet 6061/7075 VR38 Billet dry/wet engine block. Magnus Motorsports, Canada. <https://www.magnusmotorsports.com/product/magnus-billet-6061-7075-vr38-billet-dry-wet-engine-block> (accessed on 30.05.2023).
- [14] Metals – Brinell hardness measurement, part 1: test method. Standard EN ISO 6506-1:2014-12. PKN; 2014.
- [15] Przybyłowicz K. Metallography (in Polish). Wydawnictwa Naukowo-Techniczne. Warsaw 1996.
- [16] Rose GJ, Venkatesan H, Arijit MK, Lindsay SRK, Premkumar TM, Development of automotive cam shaft using aluminium – silicon carbide composite – an effectiveness study. *Mater Today-Proc*. 2023;72:2108-2112. <https://doi.org/10.1016/j.matpr.2022.08.220>
- [17] Sachar S, Parvez Y, Khurana T, Chaubey H. Heat transfer enhancement of the air-cooled engine fins through geometrical and material analysis: a review. *Mater Today-Proc*. 2023 (in press). <https://doi.org/10.1016/j.matpr.2023.03.447>
- [18] Sajadifar S, Suckow T, Chandra K, Heider B, Heidazageh A, Zavasnik J et al. Assessment of the impact of process parameters on the final material properties in forming of AW 7075 employing a simulated forming process. *J Manuf Process*. 2023;86:336-353. <https://doi.org/10.1016/j.jmapro.2022.12.056>
- [19] Siadkowska K, Czyż Z. Selecting a material for an aircraft diesel engine block. *Combustion Engines*. 2019;178(3):4-8. <https://doi.org/10.19206/CE-2019-301>
- [20] Standard test method for crack-tip opening displacement (CTOD) fracture toughness measurement. Standard ASTM E1290-08 (E01). ASTM 2008.
- [21] Trdan U, Klobcar D, Berthe L, Sturm R, Bergant Z. High-cycle fatigue enhancement of dissimilar 2017A-T451/7075-T651 Al alloy joint fabricated by a single pass FSW without

- any post-processing. *J Mater Res Technol.* 2023;25:2333-2352. <https://doi.org/10.1016/j.jmrt.2023.06.096>
- [22] Wieszała R. Characteristics of car structures made of aluminum alloys. *Ores and non-ferrous metals recycling* (in Polish). SIGMA-NOT Publishing House. 2014;59(10):497-501.
- [23] Zakrzewski M, Zawadzki J. *Strength of materials* (in Polish). Państwowe Wydawnictwo Naukowe. Warsaw 1983.
- [24] Zheng R. *Mechanical properties of 7075 aluminium matrix composites reinforced by nanometric silicon carbide particulates*. Master thesis. University of New South Wales Sydney 2007.

Grzegorz Chruścielski, DEng. – Department of Automotive Engineering, Wrocław University of Science and Technology, Poland.

e-mail: grzegorz.chruscielski@pwr.edu.pl



Robert Jasiński, DEng. – Department of Automotive Engineering, Wrocław University of Science and Technology, Poland.

e-mail: robert.jasinski@pwr.edu.pl

